Journal of Alloys and Compounds, 206 (1994) 133–139
JALCOM 999

On the order and disorder of the transition metal (T) and silicon atoms in ternary thorium transition metal silicides of the compositions Th_2TSi_3 and ThTSi

Jörg H. Albering
Anorganisch-Chemisches Institut, Universität Münster, Wilhelm-Klemm-Strasse 8, D-48149 Münster (Germany)

Rainer Pöttgen and Wolfgang Jeitschko
Anorganisch-Chemisches Institut, Universität Münster, Wilhelm-Klemm-Strasse 8, D-48149 Münster (Germany), and Laboratoire de Chimie du Solide du CNRS, Université de Bordeaux I, 351 Cours de la Libération, F-33405 Talence Cedex (France)

Rolf-Dieter Hoffmann
Anorganisch-Chemisches Institut, Universität Münster, Wilhelm-Klemm-Strasse 8, D-48149 Münster (Germany)

Bernard Chevalier and Jean Etourneau
Laboratoire de Chimie du Solide du CNRS, Université de Bordeaux I, 351 Cours de la Libération, F-33405 Talence Cedex (France)

(Received October 16, 1993)

Abstract

During phase investigations of the ternary systems thorium–transition metal–silicon, 12 ternary thorium transition metal silicides Th_2TSi_3 (T ≡ Mn, Fe, Co, Ni, Cu, Ru, Rh, Pd, Os, Ir, Pt, Au), nine of them for the first time, were prepared by arc melting of the elemental components and subsequent annealing. The silicides with Co, Ni and Cu crystallize with a hexagonal AlB_2-type structure, while all other compositions adopt the tetragonal structure of α-$ThSi_2$. Although it can be assumed that the transition metal and silicon atoms occupy the boron and silicon positions of AlB_2 and α-$ThSi_2$ with at least some short-range order, no evidence for an ordered occupancy of these positions was found. In contrast, in the new equiatomic compound ThAuSi the gold and silicon atoms occupy the boron positions of AlB_2 in an ordered manner. There is a principal difference for compounds with order–disorder transitions depending on whether the ordering results in a translationengleiche or a klassengleiche subgroup. For structures with a translationengleiche subgroup the order changes the intensities of the reflections already present in the disordered structure, while for ordered structures with klassengleiche subgroups the order can be detected only through the observation of superstructure reflections.

1. Introduction

Thorium forms two silicides of the composition $ThSi_2$ [1–4]: a tetragonal α form with a structure first determined for this compound and a hexagonal β form which is isotypic with AlB_2. In addition, a defect AlB_2-type structure with a different c/a ratio was reported for Th_3Si_5 [2]. Both forms of the disilicide are superconducting at $T_{cr} = 3.16$ K (α-$ThSi_2$) and $T_{cr} = 2.41$ K (β-$ThSi_2$) respectively [5]. They form solid solutions ThT_xSi_{2-x} (T ≡ Co, Ni, Rh, Ir, Pt) by replacing some percentage of the silicon atoms by transition metal atoms. These five series were intensively investigated in Bordeaux [6–8] when searching for new superconducting materials.

During the last years a new family of ternary silicides U_2TSi_3 (T ≡ Mn, Fe, Co, Ni, Cu, Ru, Rh, Pd, Os, Ir, Pt, Au) [9–16] was prepared and characterized. These compounds also crystallize either with a hexagonal AlB_2-type or a tetragonal α-$ThSi_2$-type structure. For U_2RuSi_3 and U_2OsSi_3 a new ordered version of an AlB_2-type structure was observed recently [17].

We were interested in the corresponding thorium compounds and investigated several ternary systems thorium–transition metal–silicon. In the present paper we report on the synthesis of nine new compositions Th_2TSi_3 (T ≡ Mn, Fe, Ni, Cu, Ru, Pd, Os, Pt, Au) and on the new equiatomic silicide ThAuSi.

0925-8388/94/$07.00
SSDI 0925-8388(93)00999-F

2. Experimental details

Starting materials for the preparation of the ternary silicides were high purity thorium ingots (greater than 99.9%), powders of the transition metals (all with nominal purities greater than 99.9%) and silicon powder (Merck, greater than 99.9%). Thorium filings were prepared under dried paraffin oil. They were washed with dried cyclohexane under argon and were not allowed to contact air prior to the reactions.

The samples were prepared by arc melting of small (about 400 mg) cold-pressed pellets of the elemental components of the intended composition in an argon (99.996%) atmosphere. The argon was further purified by repeatedly melting a titanium button prior to the reactions. The buttons were flipped over and remelted several times to ensure good homogeneity. Subsequently the samples were annealed in evacuated sealed silica tubes at 800 °C for 1 week. The weight loss of the samples after several meltings was always smaller than 1%.

All the crushed buttons had a light grey colour with metallic lustre. They were stable in air and no decomposition was visible after several months.

The samples were characterized by Guinier powder diagrams using Cu $K\alpha_1$ radiation and α-quartz ($a = 491.30$ pm, $c = 540.46$ pm) as an internal standard. The lattice constants were obtained by least-squares fits of the powder data.

The powder diffractometer measurement of the ThAuSi sample was performed on a Stoe STADI/P focusing monochromatic beam diffractometer with a rotating sample in the symmetric transmission mode. Cu $K\alpha_1$ radiation was used with a linear photosensitive detector, a step width of 0.02° (2θ) and a constant counting time of 20 s per step. The intensities of this diffraction pattern were obtained with the aid of the RIETAN programme [18].

Density measurements of the ternary samples $ThAu_xSi_{2-x}$ were carried out at room temperature with a conventional pycnometer using petroleum ($\rho = 0.767$ g cm^{-3}) as the liquid phase.

3. The series with the composition Th_2TSi_3

The lattice constants of the 12 silicides with the composition Th_2TSi_3 are listed in Table 1. The compounds with Co, Ni and Cu adopt a hexagonal AlB_2-type structure, while the others crystallize with the tetragonal structure of α-$ThSi_2$. To ensure the proper identification of the phases, intensity calculations for the Guinier powder data were carried out using the positional parameters of the AlB_2- and α-$ThSi_2$-type structures assuming a statistical distribution of 25% transition metal and 75% silicon atoms on the B and Si positions of AlB_2 and α-$ThSi_2$. The evaluations of the powder diagrams for Th_2MnSi_3 and Th_2OsSi_3 are shown as examples in Table 2.

We tried to synthesize a silver-containing sample with the composition Th_2AgSi_3; however, because of the low boiling point of silver, such samples always showed a large weight loss during the arc-melting process. The powder diagrams of these samples showed the diffraction lines of an AlB_2-type cell; however, the lattice constants were close to those of the binary

TABLE 1. Lattice constants of the binary and ternary silicides with hexagonal AlB_2- and tetragonal α-$ThSi_2$-type structures[a]

Compound	Structure type	a (pm)	c (pm)	c/a	V (nm^3)	Reference
β-$ThSi_2$	AlB_2	413.6(1)	412.6(1)	0.998	0.0611	2
Th_3Si_5	AlB_2	398.5(1)	422.8(1)	1.061	0.0581	2
Th_2CoSi_3	AlB_2	405.2(2)	415.1(1)	1.024	0.0590	This work
Th_2CoSi_3	AlB_2	404.3	418.9	1.036	0.0593	7
Th_2NiSi_3	AlB_2	403.22(7)	418.90(6)	1.039	0.0590	This work
Th_2CuSi_3	AlB_2	402.3(1)	419.1(1)	1.042	0.0588	This work
α-$ThSi_2$	α-$ThSi_2$	412.7	1419.4	3.440	0.2418	7
Th_2MnSi_3	α-$ThSi_2$	410.69(7)	1411.3(3)	3.436	0.2380	This work
Th_2FeSi_3	α-$ThSi_2$	409.93(8)	1418.5(4)	3.460	0.2384	This work
Th_2RuSi_3	α-$ThSi_2$	412.42(5)	1444.7(3)	3.503	0.2457	This work
Th_2RhSi_3	α-$Thsi_2$	412.41(7)	1438.7(3)	3.489	0.2447	This work
Th_2RhSi_3	α-$ThSi_2$	411.7	1431	3.476	0.2426	8
Th_2PdSi_3	α-$ThSi_2$	415.70(5)	1428.2(3)	3.436	0.2468	This work
Th_2OsSi_3	α-$ThSi_2$	413.84(4)	1437.4(3)	3.473	0.2462	This work
Th_2IrSi_3	α-$ThSi_2$	413.66(7)	1436.4(4)	3.472	0.2458	This work
Th_2IrSi_3	α-$ThSi_2$	412	1432	3.476	0.2431	8
Th_2PtSi_3	α-$ThSi_2$	415.92(3)	1428.5(2)	3.435	0.2471	This work
Th_2AuSi_3	α-$ThSi_2$	419.72(7)	1430.3(4)	3.408	0.2520	This work

[a]Standard deviations in the positions of the least significant digits are given in parentheses throughout the paper.

TABLE 2. Guinier powder patterns of Th_2MnSi_3 and Th_2OsSi_3 with a tetragonal α-$ThSi_2$-type structure[a]

Th_2MnSi_3					Th_2OsSi_3				
hkl	Q_c	Q_o	I_c	I_o	*hkl*	Q_c	Q_o	I_c	I_o
101	643	642	45	s	101	632	632	15	m
004	803	802	25	s	004	774	774	14	s
103	1045	1043	52	s	103	1019	1019	42	s
112	1387	1385	100	vs	112	1361	1359	100	vs
105	1848	1846	42	m	105	1794	1792	47	s
200	2372	2371	32	m	200	2336	2334	37	s
202	2572	–	<1	–	202	2529	–	<1	–
116	2993	2991	12	m	116	2910	2909	13	w
211	3015	3015	13	w	107	2955	2956	24	m
107	3053	3053	21	w	211	2968	–	5	–
204	3175	3174	17	m	008	3097	–	2	–
008	3213	–	4	–	204	3110	3109	10	m
213	3416	3418	22	m	213	3355	3353	17	m
206	4179	–	<1	–	206	4078	–	<1	–
215	4220	4221	28	m	215	4129	4128	31	m
109	4659	4661	8	vw	109	4504	4505	6	vw

[a]The patterns were recorded in a Guinier camera with Cu $K\alpha_1$ radiation. The Q values are defined by $Q = 100/d^2$ (nm^{-2}). Intensities were calculated using the LAZY-PULVERIX programme [19] assuming the positional parameters of the α-$ThSi_2$ structure with 25% T and 75% Si on the silicon positions. The observed intensities I_o from very weak to very strong are abbreviated by vw, w, m, s, vs.

compound Th_3Si_5 [2]. Thus we conclude that the samples had a low silver content even though a binary phase $ThAg_2$ with AlB_2-type structure is known to exist [4]. Similar results were obtained when we tried to prepare the corresponding uranium sample U_2AgSi_3. The lattice constants of these samples were in agreement with those of U_3Si_5 [2].

4. The pseudobinary system $ThAu_2$–$ThSi_2$

For the ternary system thorium–gold–silicon the whole pseudobinary section $ThAu_2$–$ThSi_2$ was investigated. The powder diagrams of the samples $ThAu_xSi_{2-x}$ with x up to 0.7 correspond to the tetragonal α-$ThSi_2$-type structure, while the samples with $x = 0.9$ and 1.0 show a pattern similar to an AlB_2-type structure (Table 3). The samples with a higher gold content contained three phases and thus do not belong to the pseudobinary system. For the samples with the tetragonal α-$ThSi_2$-type structure the lattice constant a increases linearly from 412.7 pm (α-$ThSi_2$) to 420.5 pm ($ThAu_{0.7}Si_{1.3}$). In contrast, the lattice constant c first decreases very slightly from 1419.4 pm (α-$ThSi_2$) to 1417.6 pm ($ThAu_{0.2}Si_{1.8}$) and then increases to 1449.5 pm ($ThAu_{0.7}Si_{1.3}$). The increase in both lattice constants is certainly due to the larger metallic radius of the gold atoms (144 pm as compared with 132 pm for silicon, both for the coordination number 12 [20]). We also measured the pycnometric densities of these samples. They agree very well with the calculated ones (Table 3). This excludes the formation of defects as is known for the AlB_2-type structure of Th_3Si_5 [2]. The densities increase with increasing gold content in a linear fashion (Fig. 1) and this linearity can be extrapolated up to the binary compound $ThAu_2$ [4], which also crystallizes in the AlB_2-type structure.

The samples with $x = 0.9$ and 1.0 show hexagonal symmetry and the diffraction patterns suggest an AlB_2-type atomic arrangement. Intensity calculations for the equiatomic composition ThAuSi showed that the gold and silicon atoms occupy the boron positions in this hexagonal cell in an ordered arrangement. The residual values of $R = 0.026$ for the ordered and $R = 0.093$ for the random distribution of the gold and silicon atoms on the boron positions of AlB_2 clearly favour the structure with the ordered arrangement. These residuals, defined by $R = \Sigma|I_o - I_c|/\Sigma I_o$, were calculated from the intensities listed in Table 4 and do not result from least-squares fits of the data. Thus the structure, as shown in Fig. 2, can be described in the space group $P\bar{6}m2$ (No. 187) with the positional parameters and interatomic distances of Table 5.

5. Discussion

Of the 12 compositions Th_2TSi_3 prepared in the present investigation (Table 1), the nine with T ≡ Mn,

TABLE 3. Lattice constants and densities ρ of the silicides $ThAu_xSi_{2-x}$

Compound	Structure type	a (pm)	c (pm)	c/a	V (nm^3)	ρ_{calc} (g cm^{-3})	ρ_{exp} (g cm^{-3})	Reference
$ThSi_2$	α-$ThSi_2$	412.7	1419.4	3.440	0.2418	7.71	7.63	3, 7
$ThAu_{0.2}Si_{1.8}$	α-$ThSi_2$	414.65(4)	1417.6(2)	3.419	0.2437	8.78	8.4(1)	This work
$ThAu_{0.4}Si_{1.6}$	α-$ThSi_2$	417.50(5)	1422.7(2)	3.408	0.2480	9.53	9.2(1)	This work
Th_2AuSi_3	α-$ThSi_2$	419.71(7)	1430.3(3)	3.408	0.2520	9.82	10.0(1)	This work
$ThAu_{0.7}Si_{1.3}$	α-$ThSi_2$	420.50(4)	1449.5(2)	3.447	0.2563	10.53	10.5(1)	This work
$ThAu_{0.9}Si_{1.1}$	AlB_2	425.9(3)	417.3(2)	0.980	0.0655	11.16	11.1(1)	This work
ThAuSi	LiBaSi	426.0(3)	416.4(4)	0.977	0.0655	11.59	11.7(1)	This work
$ThAu_2$	AlB_2	474.0(2)	340.2(2)	0.718	0.0662	15.75	15.35	4

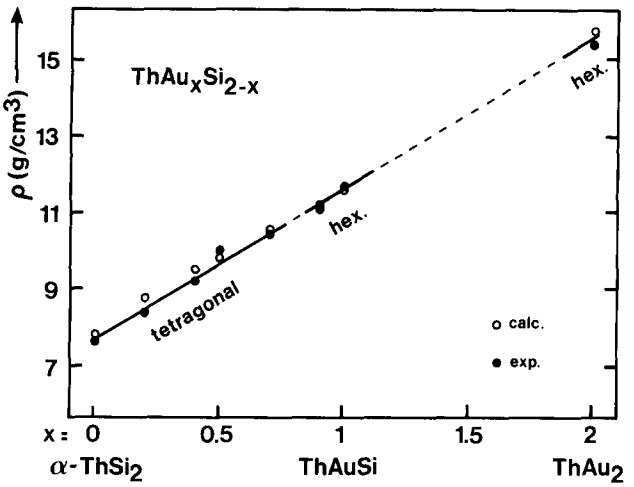

Fig. 1. Observed and calculated densities of the solid solutions $ThAu_xSi_{2-x}$.

TABLE 4. X-Ray powder data for ThAuSi. The pattern was recorded with Cu $K\alpha_1$ radiation. The last two columns list the calculated intensities assuming ordered and disordered distributions of the Au and Si atoms on the boron sites of AlB_2

hkl	$2\theta_{obs}$	$2\theta_{calc}$	*d* (Å)	I_{obs}	I_{calc} (order)	I_{calc} (disorder)
001	21.35	21.31	4.168	1	1	1
100	24.26	24.22	3.673	242	277	128
101	32.51	32.47	2.756	1000	1000	1000
110	42.65	42.61	2.121	359	354	394
002	43.44	43.40	2.084	113	112	124
111	48.15	48.11	1.890	<1	<1	<1
200	49.65	49.61	1.837	31	32	27
102	50.35	50.31	1.813	77	80	53
201	54.61	54.57	1.681	218	233	224
112	62.48	62.44	1.486	223	234	232
003	67.39	67.36	1.389	<1	<1	1
210	67.45	67.42	1.388	34	34	29
202	68.03	68.00	1.378	26	26	29
211	71.63	71.60	1.317	204	204	191
103	72.76	72.73	1.299	98	98	92
300	78.02	77.99	1.224	63	61	56
301	81.99	81.97	1.175	<1	<1	<1
113	83.08	83.06	1.162	<1	<1	<1
212	83.67	83.65	1.155	39	38	40
203	88.14	88.11	1.108	62	62	55
220	93.23	93.21	1.060	41	40	35
302	93.77	93.75	1.056	80	81	69
004	95.38	95.37	1.042	13	13	11
221	97.16	97.14	1.028	<1	<1	9
310	98.29	98.27	1.019	10	10	18
					$R=0.026$	$R=0.093$

Fe, Ni, Cu, Ru, Pd, Os, Pt and Au are reported here for the first time. The compounds with Co, Ni and Cu adopt the hexagonal AlB_2-type structure, while the others crystallize in the tetragonal structure of α-$ThSi_2$. This is in contrast with the corresponding uranium compounds, where only U_2CuSi_3 [13–15] adopts the

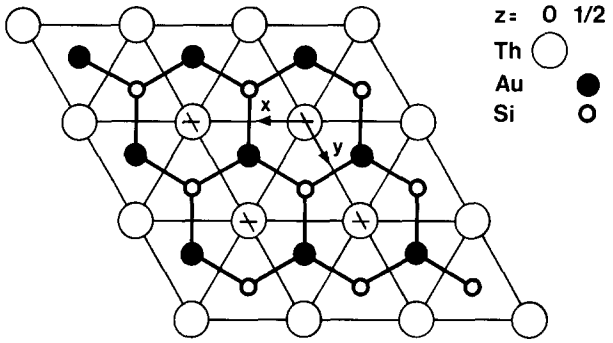

Fig. 2. Crystal structure of ThAuSi projected along the *z* direction. All atoms are situated on mirror planes at $z=0$ and $\frac{1}{2}$ connected by thin and thick lines respectively.

TABLE 5. Positional parameters and interatomic distances (picometres) of ThAuSi

Atom	*P*$\tilde{6}$*m*2	*x*	*y*	*z*
Th	1*a*	0	0	0
Au	1*f*	$\frac{2}{3}$	$\frac{1}{3}$	$\frac{1}{2}$
Si	1*d*	$\frac{1}{3}$	$\frac{2}{3}$	$\frac{1}{2}$

Th–6 Au	322.3(3)	Au–3 Si	246.0(2)	Si–3 Au	246.0(2)
6 Si	322.3(3)	6 Th	322.3(3)	6 Th	322.3(3)
2 Th	416.4(4)				
6 Th	426.0(3)				

tetragonal α-$ThSi_2$-type structure, while the others crystallize in the hexagonal structure of AlB_2. Considerable homogeneity ranges may be assumed for these phases and those with the tetragonal α-$ThSi_2$-type structure may form continuous series of solid solutions with the binary phase α-$ThSi_2$, as was shown already for the series $ThRh_xSi_{2-x}$ and $ThIr_xSi_{2-x}$ [6, 8]. At temperatures above 1350 °C α-$ThSi_2$ transforms to the β form [4] and similar transformations with temperature and/or pressure may be assumed to occur also for the ternary compositions Th_2TSi_3 reported here.

Of the pseudobinary systems α-$ThSi_2$–ThT_2, most information is available for the systems with T ≡ Co, Ni, Rh, Ir, Pt and Au. In Fig. 3 we give a summary of the structures occurring in these pseudobinary systems. It can be seen that a change in structure occurs quite frequently and the system with nickel even has two phases with α-$ThSi_2$- and two with AlB_2-type structure at relatively low temperatures (the samples of Th_2NiSi_3 and ThNiSi were annealed at 800 and 950 °C respectively). At higher temperatures other equilibria may exist. In fact, for the systems with nickel and gold it seems possible that continuous solid solutions with AlB_2-type structure might form at very high temperatures, since above 1350 °C $ThSi_2$ has the hexagonal AlB_2-type structure like $ThNi_2$ and $ThAu_2$. Furthermore,

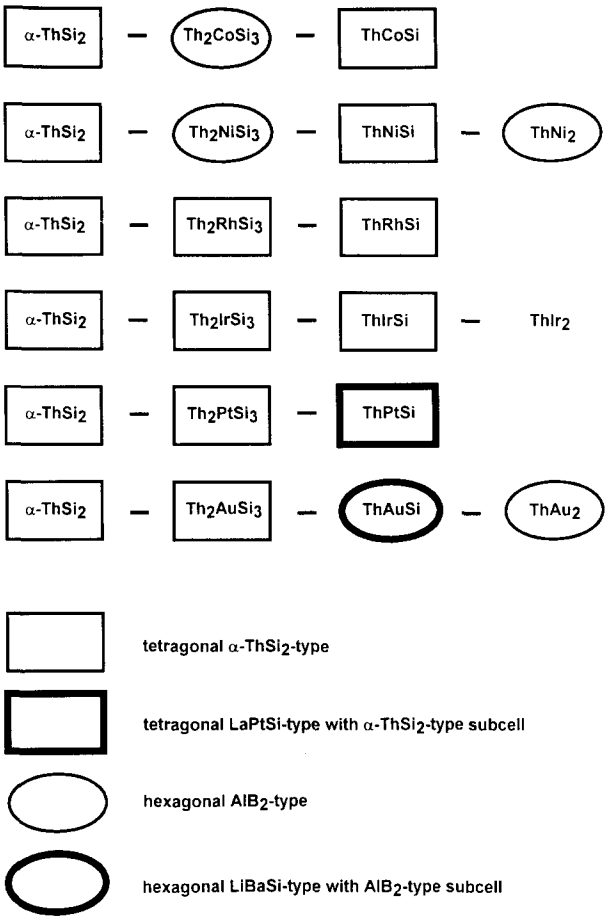

Fig. 3. Crystal structures occurring for certain compositions of the pseudobinary sections α-$ThSi_2$–ThT_2.

it is frequently observed that at higher temperatures the structures with the smaller cell volumes and higher symmetry (smaller number of positional parameters) are favoured, *i.e.* the AlB_2-type structure is favoured for the ternary compositions also for these reasons.

For ThAuSi we have established a structure deriving from that of AlB_2 with an ordered arrangement of the Au and Si atoms on the boron positions of AlB_2. Thus the Au and Si atoms alternate within the graphite-like nets, as is known for the hexagonal modification of BN. The atomic positions of ThAuSi, as we described them in Table 5, correspond to those of LiBaSi [21] and SrPtSb [22], where Li, Si, Pt and Sb atoms occupy the boron positions of AlB_2 in an ordered manner.

A similar structure with a doubled *c* axis was reported recently for ScAuSi and LuAuSi [23]. In these silicides the doubling of the *c* axis is solely a result of a slight puckering of the BN-type AuSi layers. Such puckered nets also occur in the LiGaGe-type structure [24] of YAuSi [23]. In this latter structure the doubling of the *c* axis additionally results from the alternating arrangement of the Au and Si atoms when viewed along the *c* axis. While we can rule out an LiGaGe-type structure for ThAuSi right away – because in the AlB_2-type subcell of such a structure the Au and Si atoms again would be statistically distributed – we cannot exclude a slight puckering of the AuSi nets of the type found for ScAuSi and LuAuSi in ThAuSi. The superstructure reflections (resulting from the doubled *c* axis) for such a structure would be very weak and hardly visible in a powder pattern. In fact, no such superstructure lines could be detected in the pattern of ThAuSi. However, a comparison of the Au–Si distances at first sight slightly favours a puckered arrangement also for ThAuSi. In the puckered AuSi nets of ScAuSi, YAuSi and LuAuSi these distances are 249(1), 249(1) and 252(1) pm respectively. Thus they are all slightly greater than the distance of 246.0(3) pm calculated from the positional parameters of ThAuSi as given in Table 5, and longer Au–Si distances would result if the AuSi nets were puckered. However, the Au–Si bond distances of the four structures do not need to be the same, because Th certainly will contribute four valence electrons per formula unit to the band structure, while Sc, Y and Lu can only contribute three. In the absence of any hard evidence for the puckering of the AuSi nets in ThAuSi we therefore favour the simpler description of the structure as given in Table 5.

For the equiatomic silicide compositions ThTSi of Fig. 3 with a tetragonal α-$ThSi_2$-type structure an ordered arrangement of the T and Si atoms on the silicon positions of α-$ThSi_2$ has been established so far only for ThPtSi [7], which was found to be isotypic with LaPtSi [25]. No conclusive evidence for such an atomic order was found for the compositions with T ≡ Co, Rh, Ir and Ni; nevertheless, it was not ruled out [7]. Actually, in view of the presently available evidence, we expect at least short-range order for all these compositions.

For the silicides with the composition 2:1:3 two closely related superstructures were found, both with AlB_2-type subcells. One of these was reported for Er_2RhSi_3 [26, 27] and the rare earth (RE) transition metal silicides with the compositions RE_2RhSi_3 [26] and RE_2PdSi_3 [28] are believed to be isotypic with Er_2RhSi_3. In this structure both the *a* and the *c* axis of the AlB_2-type subcell are doubled. For the other superstructure, investigated only recently for U_2RuSi_3 [17], only the *a* axis of the AlB_2-type subcell was established to be doubled, whereas no evidence for the doubling of the *c* axis could be detected. Both structures have similar atomic positions with TSi_3 nets as shown in the right-hand part of Fig. 4. The doubling of the *c* axis in Er_2RhSi_3 results from slight distortions of the U_2RuSi_3 structure and possibly both of these structures occur for several of the 2:1:3 silicides, the higher symmetry U_2RuSi_3-type structure at high temperatures and

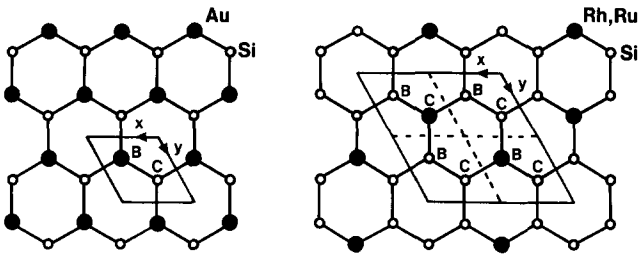

Fig. 4. Two-dimensionally infinite transition metal–silicon networks $(AuSi)_n$ and $(TSi_3)_n$ in the structures of ThAuSi and Er_2RhSi_3 [26, 27] as well as U_2RuSi_3 [17]. While the gold atoms are on the B positions of ThAuSi with ordered AlB_2 (LiBaSi)-type structure, the rhodium and ruthenium atoms of Er_2RhSi_3 and U_2RuSi_3 occupy the B and C positions of the AlB_2-type subcells (dashed lines) in equal amounts.

the lower symmetry Er_2RhSi_3-type structure at low temperatures.

In the present investigation we have found the samples Th_2TSi_3 (T ≡ Co, Ni, Cu) to crystallize with an AlB_2-type structure. We had expected some order for the transition metal and silicon atoms on the boron sites of the AlB_2-type cell. However, no evidence for a superstructure could be detected even though the samples were annealed for 1 week at 800 °C. We have calculated powder patterns assuming ordered arrangements of the types found for Er_2RhSi_3 and U_2RuSi_3, and these show that the scattering powers of the transition metal atoms Co, Ni and Cu are too similar to that of silicon to produce well-visible superstructure reflections in the presence of the strongly scattering thorium atoms. Also, one has to keep in mind that sharp superstructure reflections can develop only for samples with exactly the composition 2:1:3. Slight deviations from this ideal composition may prevent long-range order and thus broaden the superstructure reflections, which makes them even less visible.

This is different for the atomic order of the LiBaSi type found for ThAuSi, where the order expresses itself already in the intensities of the AlB_2-type subcell reflections. For an atomic order of the type found for Er_2RhSi_3 and U_2RuSi_3 the intensities of the AlB_2-type subcell remain unchanged, since the transition metal and silicon atoms are occupying the B and C positions (Fig. 4) of the AlB_2-type subcell in equal amounts. Thus there is a principal difference between the two cases. For both cases the ordering of the transition metal and silicon atoms on the boron positions of the AlB_2-type subcell (space group *P6/mmm*, crystal class *6/mmm*) results in a reduction of the symmetry. In the case of the LiBaSi-type ordered structure (space group $P\bar{6}m2$, crystal class $\bar{6}m2$) the translational symmetry does not change. The ordering results in a "*translationengleiche*" subgroup [29] and expresses itself already in the intensities of the subcell reflections. In the other case of the Er_2RhSi_3- (space group $P6_3/mmc$, crystal class *6/mmm*) and U_2RuSi_3-type (space group *P6/mmm*, crystal class *6/mmm*) superstructures the translational symmetry is changed (hence the name "super"structure) and the crystal class has not changed. The ordering results in a "*klassengleiche*" subgroup and can be detected only through the occurrence of superstructure reflections. To our knowledge this principal difference in (potential) order–disorder transitions has not been emphasized before. In the classical cases of order–disorder transitions (Cu_3Au, CuZn) the ordering results always in "*klassengleiche*" subgroups and superstructure reflections.

For the other compositions 2:1:3 with the tetragonal α-$ThSi_2$-type structure we also could not find any superstructure reflections, although at least some short-range order can be expected. For this subcell a superstructure was established up to now only for the composition 1:1:1 with the LaPtSi-type structure [25], as already mentioned. We think that it might be worthwhile to investigate the whole pseudobinary sections of these ternary systems also at different temperatures and pressures to obtain more information about the relative stabilities of the AlB_2- and α-$ThSi_2$-type structures and the ordering of the transition metal and silicon atoms.

Acknowledgments

We thank K. Wagner for the collection of the powder diffractometer data of ThAuSi. We also acknowledge Dr. W. Gerhartz (Degussa AG.) and Dr. G. Höfer (Heraeus Quarzschmelze) for generous gifts of platinum metals and silica tubes. We are grateful to the Fonds der Chemischen Industrie for a stipend to J.H.A. and to the European Community for a fellowship to R.P. in the framework of the "Human Capital and Mobility Programme". This work was supported by the Deutsche Forschungsgemeinschaft.

References

1 E.L. Jacobsen, R.D. Freeman, A.G. Tharp and A.W. Searcy, *J. Am. Chem. Soc., 78* (1956) 4850.
2 A. Brown and J.J. Norreys, *Nature, 183* (1959) 673.
3 G. Brauer and A. Mitius, *Z. Anorg. Allg. Chem., 249* (1942) 325.
4 A. Brown, *Acta Crystallogr., 14* (1961) 860.
5 G.F. Hardy and J.K. Hulm, *Phys. Rev., 93* (1954) 1004.
6 P. Lejay, B. Chevalier, J. Etourneau, J.M. Tarascon and P. Hagenmuller, *Mater. Res. Bull., 18* (1983) 67.
7 W.X. Zhong, W.L. Ng, B. Chevalier, J. Etourneau and P. Hagenmuller, *Mater. Res. Bull., 20* (1985) 1229.

8 B. Chevalier, W.X. Zhong, B. Buffat, J. Etourneau, P. Hagenmuller, P. Lejay, L. Porte, T.M. Duc, M.J. Besnus and J.P. Kappler, *Mater. Res. Bull., 21* (1986) 183.
9 M. de Lourdes Pinto, *Acta Crystallogr., 21* (1966) 999.
10 C. Geibel, C. Kämmerer, E. Göring, R. Moog, G. Sparn, R. Henseleit, G. Cordier, S. Horn and F. Steglich, *J. Magn. Magn. Mater., 90–91* (1990) 435.
11 N. Sato, M. Kagawa, K. Tanaka, N. Takeda, T. Satoh, S. Sakatsume and T. Komatsubara, *J. Phys. Soc. Jpn., 60* (1991) 757.
12 N. Sato, M. Kagawa, K. Tanaka, N. Takeda, T. Satoh and T. Komatsubara, *J. Magn. Magn. Mater., 108* (1992) 115.
13 D. Kaczorowski, H. Noël and R. Pöttgen, *Abstracts 23ièmes Journées des Actinides, Schwarzwald, 1993.*
14 R. Pöttgen and D. Kaczorowski, *J. Alloys Comp., 201* (1993) 157.
15 D. Kaczorowski and H. Noël, submitted to *Z. Phys. B.*
16 E. Hickey, *Thesis 803,* University of Bordeaux I, 1992.
17 R. Pöttgen, P. Gravereau, B. Darriet, B. Chevalier, E. Hickey and J. Etourneau, *J. Mater. Chem.,* in press.
18 F. Izumi, *J. Crystallogr. Soc. Jpn., 27* (1985) 23.
19 K. Yvon, W. Jeitschko and E. Parthé, *J. Appl. Crystallogr., 10* (1977) 73.
20 E. Teatum, K. Gschneidner and J. Waber, *Rep. LA-2345,* 1960 (US Department of Commerce, Washington, DC).
21 H. Axel, K.H. Janzon, H. Schäfer and A. Weiss, *Z. Naturf. B, 23* (1968) 108.
22 G. Wenski and A. Mewis, *Z. Anorg. Allg. Chem., 535* (1986) 110.
23 M.L. Fornasini, A. Iandelli and M. Pani, *J. Alloys Comp., 187* (1992) 243.
24 W. Bockelmann, H. Jacobs and H.-U. Schuster, *Z. Naturf. B, 25* (1970) 1305.
25 K. Klepp and E. Parthé, *Acta Crystallogr. B, 38* (1982) 1105.
26 B. Chevalier, P. Lejay, J. Etourneau and P. Hagenmuller, *Solid State Commun., 49* (1984) 753.
27 R.E. Gladyshevskii, K. Cenzual and E. Parthé, *J. Alloys Comp., 189* (1992) 221.
28 P.A. Kotsanidis, J.K. Yakinthos and E. Gamari-Seale, *J. Magn. Magn. Mater., 87* (1990) 199.
29 H. Wondratschek and W. Jeitschko, *Acta Crystallogr. A, 32* (1976) 664.